

The lower limit of  $t_d$  is established by considering the relation  $t_d = 2L/R_a$ . It is noted that  $R_a$ , for conditions of present interest, is approximately constant with a value near  $5 \times 10^{-2}$  ohms. Accordingly, the lower limit of  $t_d$  is set virtually by the lower limit of  $L$ . For practical reasons,  $L \geq 10$  microhenry, which is representative of the residual self-inductance in a network where the different components must be adequately deployed for cooling by radiation. Thus,  $t_d \geq 4$  msec, and this lower limit is relatively insensitive to other experimental conditions.

Numerical results may be obtained when appropriate values are assigned to some of the many parameters of the problem. The values in Table 1 appear reasonable.<sup>1</sup> With these assumed values, some characteristics of an optimized pulsed MPD system may be obtained, with  $J$  as the independent variable. This is done in Table 2 as follows:  $I_{sp}^*$ , given by (8) is used in (3). This establishes a relation between  $J$  and  $e$ , and for given values of  $J$ , results may be obtained for the first three columns of Table 2. The following columns are obtained by applying previously discussed relations.

The last two columns of Table 2 reveal that a pulsed MPD system improves rapidly as  $J$  increases, at small values, but the rate of improvement declines at higher values. Other important system parameters are determined according to previously discussed relations, provided that the associated constraints are not violated. In fact, these constraints limit the performance of the pulsed MPD system to a level not higher than that corresponding to the 30 kampf entry of Table 2. For this entry,  $N$  will have the lowest allowed value of  $3 \times 10^6$ ,  $t_d$  will be about 11 msec, and  $C$  and  $L$  will be  $\sim 1.3$  farad and  $\sim 24$  microhenry, respectively. For higher currents, either the required  $t_d$  is unacceptably short, or relation (10) is violated. Note that for this 30 kampf case, the overall efficiency is about 60% and the minimized system mass is 1750 lb.

A comparison of pulsed and steady MPD systems is best made by considering Eq. (9) for the pulsed system, and writing a similar equation with primed symbols for the steady system; then the following result is obtained when the two equations are divided:

$$M_o/M'_o = (fe'_o/e_o)^{1/2} \quad (11)$$

Parameters  $G$ ,  $t_i$  and  $m_s$  do not appear because they must be identical in both systems, if the comparison is to be on a common basis. Parameter  $f$ , given by (7) is approximately 2 for the pulse system, according to Table 1; the corresponding parameter is equal to unity for the steady MPD system as discussed earlier. Thus, Eq. (11) indicates that in a comparison of pulsed with steady MPD systems, the over-all efficiency of the pulsed system must be reduced by the factor  $f$ , which is the penalty that must be paid, because the necessary energy transformations in a pulsed system require components with substantial mass and with efficiencies lower than 100%. Since the highest over-all efficiency that may be expected from a pulsed system is about 60% and  $f \simeq 2$ , the best expected pulsed MPD will be superior only to steady MPD systems which have over-all efficiencies lower than 30%. Moreover, the superiority of the pulsed MPD would be rather marginal, due to the square root relationship in (11), unless the efficiency of the steady MPD is very much lower than 30%. Since the main contribution to a high value of  $f$  is made by the ratio  $m_c/m_s$ , (specific masses of the  $C$  bank and of the solar power supply), the superiority of the pulsed MPD system will remain at best marginal unless appropriate advances of the state-of-the-art force the ratio  $m_c/m_s$  to values substantially lower than the 50/44 assumed herein.

#### Reference

- 1 Malliaris, A. C., "System Requirements for Application of a Pulsed MPD Arc Jet to Electrical Propulsion," AIAA Paper 69-269, Williamsburg, Va., 1969.

## Particle Cloud Impingement Damage

A. J. LADERMAN\* AND C. H. LEWIS†  
Philco-Ford Corporation, Newport Beach, Calif.

SEVERAL studies of target damage induced by impaction of a cloud of micron-sized aluminum-oxide particles have been reported recently.<sup>1-3</sup> The results of these programs have established that, for a wide range of conditions typical of solid-propellant exhaust plumes, a debris layer forms immediately ahead of the exposed target surface, partially shielding it from subsequent impingement by oncoming particles. Furthermore, the test results, which were similar for all target materials including several metals and ablators,<sup>†</sup> indicated that a significant fraction of the incident particle kinetic energy flux can be absorbed by the impact debris with a corresponding large decrease in target damage. This effect, referred to as debris shielding or target shielding, is shown in Fig. 1 where the relative target damage, i.e., the ratio of total target mass loss  $m_T$  to total mass of incident

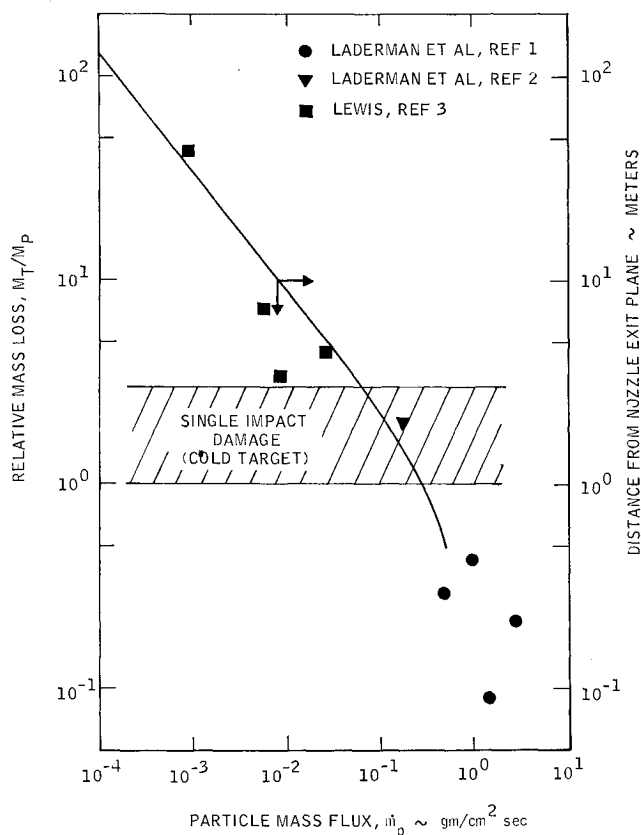


Fig. 1 Relative damage for particle cloud impingement on flat Teflon targets. The solid curve represents the particle mass flux as a function of distance from the nozzle exit plane for a typical solid-propellant rocket.

Received July 31, 1969. This work was supported by the U.S. Air Force Space and Missile Systems Organization under Contract FO4649-67-C-0051 and by NASA under JPL Contract 951246.

\* Supervisor, Experimental Fluid Physics Section, Advanced Development Operation, Aeronutronic Division. Member AIAA.

† Senior Research Engineer, Fluid Mechanics Department, Advanced Development Operation, Aeronutronic Division. Member AIAA.

‡ The metal targets included stainless steel and aluminum. The ablators were comprised of Teflon, carbon cloth phenolic, ATJ graphite, pyrolytic boron nitride, and quartz cloth phenolic which, with the exception of the latter, are pure subliming materials.

freestream particles  $m_P$  is plotted against incident particle mass flux for normal impact on flat Teflon targets. The data points, which are identified in the legend, were acquired from a cold-flow facility using helium carrier gas to accelerate the particles,<sup>1</sup> a rocket simulator facility,<sup>2</sup> and an aluminized solid-propellant rocket.<sup>3</sup> The volume mean diameter  $D_{50}$  of the particles used in the several facilities varied from 1 to  $5\mu$ , whereas the incident mean particle velocity ranged from approximately 1500 m/sec for the helium tests to 3000 m/sec for some of the simulator tests. For purposes of illustration, Fig. 1 also includes a plot of centerline particle mass flux vs axial distance from the nozzle exit plane for a typical solid-propellant rocket operating at high altitude. This curve was calculated for the following conditions: 4000 lb thrust, 500 psia chamber pressure, 25% alumina loading, and  $30^\circ$  nozzle with 40 to 1 expansion ratio. It was also assumed that at each axial station the particles uniformly fill the nozzle cone angle. For other engine sizes the particle flux can be scaled directly with the thrust level.

The scatter in the data of Fig. 1 can be attributed in part to differences in test conditions, including the shock layer gas density,<sup>§</sup> target heating, particle size, and incident particle velocity. It is significant, however, that a consistent trend is observed which indicates that target shielding persists as the particle flux changes over four orders of magnitude. In addition, it is of interest to note that as the particle mass flux becomes smaller the major constituent of the debris layer changes from spent projectile material to ejected target material. With further decrease in particle flux, it is expected that the concentration of ejecta eventually will become sufficiently dilute so that the shielding effect will vanish and the particles will impact unaltered on the target. In this case, all other factors being equal, the relative target damage should become independent of particle mass flux. Finally, it should be pointed out that the recorded damage is due principally to mechanical erosion by the impacting particles. This is clearly evidenced by the fact that, while convective gas heat transfer dominated target heating in the solid rocket tests and contributed as much as 30% of the total energy flux in the simulator experiments, the surface regression during a gas-only flow was, respectively, at least 6 and 10 times less than that observed for a two-phase flow. Furthermore, analysis of the cold-flow tests<sup>1</sup> indicates that ablation can account for only a small fraction of the observed damage.

In view of these findings it is of interest to compare the target damage described in Fig. 1 to that expected for a single impact. Reinecke<sup>4</sup> used a light gas gun to determine the damage produced by a single  $\text{SiO}_2$  particle impacting on a Teflon target initially at room temperature. For particle diameters ranging from 64 to  $73\mu$  and particle velocities of approximately 5000 m/sec, the observed mass loss ratio was 10 g of target per gram of projectile. Sorenson's<sup>5</sup> correlation of impact damage produced by metal projectiles impacting on metal targets shows that, for these projectile-target combinations, energy scaling is approximately valid for velocities as low as several km/sec. Consequently, neglecting the difference in particle size and assuming 1) that a similar relationship holds for oxide particles impacting Teflon targets and 2) that the shear strength of Teflon, which is known to be strain-rate-dependent, is roughly constant over the velocity range from 1500 to 5000 m/sec, Reinecke's data indicate a mass loss ratio of approximately

1 and 3 at projectile velocities of 1500 and 3000 m/sec, respectively. These results, shown also in Fig. 1, demonstrate that the mass loss ratio for cloud impingement can be greater or less than that for single impact, by as much as several orders of magnitude. This fact serves to illustrate the consequences of two competing processes which characterize particle cloud impingement. On one hand, the shielding effect of the debris layer reduces the particle energy below its freestream value which, in turn, tends to decrease the impact damage. On the other hand, the target heating produced either by impinging particles or by heat transfer from the surrounding gases causes a significant increase in surface temperature.<sup>1,3</sup> At elevated temperatures, the shear strength of the target is reduced, leading to greater damage than that corresponding to cold targets. The two processes are related since particle heating is controlled by the degree of shielding, which itself is dependent, in part, on the amount of material ejected from the target. Although the degree of shielding and extent of heating were not resolved in the tests reported here, Fig. 1 indicates that the magnitude of the damage depends on which process is dominant.

On the basis of the preceding discussion, it is clear that particle cloud impingement introduces several significant processes which are not associated with single impact phenomena. As a result, multiple impact damage cannot be estimated by extension of single impact data. Although the experiments to date have identified the major problem areas, further investigation is necessary before reliable methods for predicting cloud impingement damage can be established.

#### References

- <sup>1</sup> Laderman, A. J., Lewis, C. H., and Byron, S. R., "Two-Phase Plume Impingement Effects," submitted for publication to *AIAA Journal*.
- <sup>2</sup> Laderman, A. J., Lewis, C. H., and Byron, S. R., "Two-Phase Flow Impingement Forces," Final Technical Report, SAMSO TR-68-308, Aeronutronic Report U-4429, Aug. 1968, Aeronutronic Div., Philco-Ford Corp., Newport Beach, Calif.
- <sup>3</sup> Lewis, C. H., "Study of Impingement of Rocket Exhaust Gases and Solid Particles on a Spacecraft," Final Technical Report, Aeronutronic Report U-4609, JPL Contract 951246, March 1968, Aeronutronic Div., Philco-Ford Corp., Newport Beach, Calif.
- <sup>4</sup> Reinecke, W., "Some Preliminary Results Concerning the Impact of Dust-Like Micro-Particles on Teflon," presented at the IDA/ARPA Symposium on Dust, Arlington, Va., Aug. 1965.
- <sup>5</sup> Sorenson, N. R., "Systematic Investigation of Crater Formation in Metals," *Proceedings of the Seventh Symposium on Hypervelocity Impact*, Vol. VI, AD 463-232, Martin Co., Orlando, Fla., 1965, pp. 281-325.

## Ignition of Metals with $\text{ClF}_3$ and $\text{ClF}_5$ for Use as Spacecraft Chemical Heaters

ROBERT ALDEN RHEIN\*  
Jet Propulsion Laboratory,

California Institute of Technology, Pasadena, Calif.

#### Introduction

ONE of the many problems confronting a design of an unmanned spacecraft for landing on the surface of Mars is that, during the very cold Martian evenings, some

§ The shock layer gas density has an important effect on the development of the debris layer through its influence on the drag force exerted on debris particles. For the data points shown in Fig. 1, the stagnation-point gas density varied by a factor of ten while the mean value was approximately two orders of magnitude less than that of sea level air. A complete evaluation of the effects of particle drag, however, must also take into account the gas velocity and viscosity, which, in turn, depend on the composition of the gas.

Received March 24, 1969; July 22, 1969. This paper presents the results of one phase of research carried out at the Jet Propulsion Laboratory, California Institute of Technology, under Contract No. NAS 7-100, sponsored by NASA.

\* Senior Scientist.